

MEASUREMENT ERRORS RELATED TO A HAILPAD NETWORK

N. Doras  
 Groupement National d'Etudes des Fleaux Atmospheriques  
 Grenoble, France

1. INTRODUCTION

Grossversuch IV is a program designed to evaluate through statistical analysis, under a reasonably controlled condition, the efficiency of the Soviet method for hail suppression. This program was initiated in 1977 and is being carried out through cooperation between research institutes from Switzerland, France and Italy, coordinated by the Laboratory for Atmospheric Physics at E.T.H. (Zurich, Switzerland). This specifically implies operating the basic equipment necessary for applying the Soviet method (S-band radar, X-band radar, launching sites) and controlling the results (hail pads, measurement networks) within the experimental perimeter.

In Grossversuch IV, as in other experimental tests, a hailpad network is used to measure hailfall on the ground. It is therefore important to evaluate instrumental device precision concerning the global energy  $E_G$  (variable used in the test).

This precision is composed of two principal elements:

- The individual hailpad precision (point measurement errors)
- The network precision (global hail pattern measurement errors due to network sampling)

The problem of point measurement errors has already been extensively examined, particularly by Joss and Waldvogel (1969), Gertzman and Atlas (1977) and Lozowski and Strong (1978).

Important contributions concerning network sampling errors have been made by Wojtiw and Lozowski (1978), Long (1978) and by Waldvogel and Schmid (1981). Using Grossversuch IV experimental results, the study here is an attempt to establish a cumulative evaluation of these different measurement errors applicable to hailpatterns of various sizes and to several grids.

We used a simulation technique based on random superimposition of modelled hailpatterns upon a fixed network. For this, a mathematical hailpattern model had to be developed and a certain number of point measurement problems taken into consideration.

2. HAILPATTERN MODEL

To establish a hailpattern energy field model the energy density distribution was mathematically represented by a continuous function  $E(x,y)$ . The chosen form for this function is that of bivariate Gaussian:

$$E(x,y) = E_m \exp \left( -\frac{x^2}{a^2} - \frac{y^2}{b^2} \right) \quad (1)$$

This function will be zero for all points outside the hailfall area  $S_R$  defined by  $E(x,y) = \epsilon$  ( $\epsilon$  being the minimum measurable energy) and the "true" global energy as given by the integral:

$$E_R = \iint_{S_R} E(x,y) dx dy$$

The choice of this function is justified by the fact that it verifies an important experimental property established by Grossversuch IV data. The property is that of an exponential distribution of energy density in terms of the cumulative area :  $E = E_m \exp(-\mu E)$  (Mezeix and Doras, 1981). Two other experimental relations established on this occasion will be used to fix this model in maximum intensity ( $E_m$ ) and in spatial scattering (a) following the given value  $E_R$ . The relations are:

$$\begin{aligned} \mu_E &= 2.4 S_G^{-0.825} \\ S_G &= 3.47 E_G^{0.04} + 0.09 \log E_R \end{aligned} \quad (2)$$

They were established between the measured parameters  $S_G$ ,  $E_G$  and  $\mu_E$ . Using them to fix the model is the same as making the hypothesis that the "true" corresponding parameters  $S_R$ ,  $E_R$  and  $\mu$  have the same relations among themselves. This hypothesis remains valid as long as the measurement introduces no significant bias. The result obtained can be expressed as:

$$E(x,y) = \frac{0.86 E_R^{0.967-0.074 \log E_R}}{1 - \exp(-2.98 E_R^{0.007+0.016 \log E_R})} \exp - \left[ \frac{0.86 \mu}{E_R^{0.033+0.07 \log E_R}} \left( \frac{x^2}{1-e^2} + (1-e^2)y^2 \right) \right]$$

On one hand the interest of a so defined model is that it allows us to keep a realistic representation of energy density distribution regardless of the hailpattern size. On the other hand, it maintains one form of a parameter, the eccentricity  $e$ , which can be randomly varied to account for hailpattern form diversities.

Two main objections can be made concerning this type of model. First, the energy distribution is unimodal (with only one maximum) whereas

in reality certain hailpatterns have 2, even 3 or 4 separate maxima (hailcores). Second, the hailpattern fine scale variability, as measured on dense networks (Morgan and Towery, 1975), is not reflected by such an even function as  $E(x,y)$ .

### 3. MEASUREMENT SIMULATION

Using the above model and for a given "true" energy value  $E_R$ , random hailpatterns upon a fixed network can be sampled and their measured global energy  $E_T$  calculated. Then to simulate the complete natural hailfall measurement process, we have to establish the whole measured response obtained from a climatologic distribution of value  $E_R$ .

#### 3.1 Network hailfall sampling

On the network, the hailpattern position and orientation are considered to be random. For a given value  $E_R$ , a hailpattern can be completely defined when its position, orientation and eccentricity are randomly selected on the computer. This selection is done in such a way that the hailfall is situated entirely inside the network. All the P network stations hit are determined, as well as their corresponding "true" energy density values  $E(x,y)$ . To then go from these values  $E(x,y)$  to the measured energy density  $E_T$ , it is necessary to include the hailpad measurement conditions.

#### 3.2 Point measurement conditions

Causes of hailpad errors noted in Grossversuch IV are numerous. Among those evaluated as being most important are the following: hailpad statistical representativeness, hailstone speed limit hypothesis, dent measurement, calibration and eventually saturation. Another non-negligible cause of measurement error, not taken into consideration for the present simulation, is the grouping of hailstone dents into diameter classes. Most of these measurement errors are accidental and result in random variations. To integrate these variations practically into the simulation process, they will be interpreted as composed background noise to be added to the "true" value  $E(x,y)$ .

The first cause of error comes from the hailpad statistical representativeness. This problem was developed theoretically by Gertzman and Atlas (1977) with a Poisson hailstone dimensional distribution. An application of this method by Waldvogel et al (1978) to Napf plain hailfalls gives variations as a function of  $E$ . Experimentally in Grossversuch IV, the point error variation could be indicated with the help of doubled pads. For each pair of measures obtained between 1977 and 1980, Figure (1) shows the relative deviation between two energy densities in terms of their average values. This relative deviation varies considerably but remains within the continuous curve, the equation being  $Y = x^{-0.3}$ . These measurements are in agreement with the Waldvogel et al. results.

To interpret this point sampling variations, a uniform background noise of maximum amplitude  $DE = E \cdot 0.12$  is considered.

The error due to hailstone speed limit variations remains small. For a speed variation of 15%, it only produces a 6% kinetic energy variation (Mezeix and Admirat, 1978). In practice, a uniform background noise of maximum amplitude  $0.12 E$  is employed in the simulation.

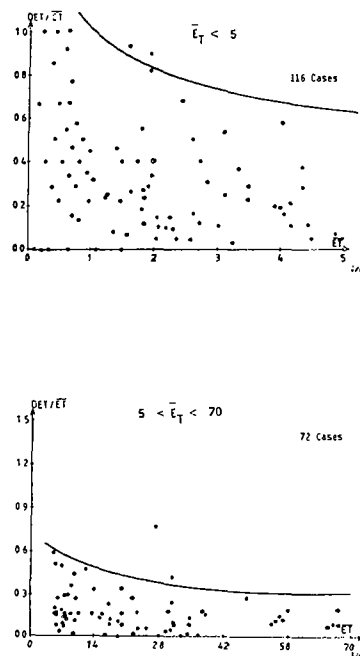


Fig. 1. Relative variations of doubled pads energy density measurement

The error due to dent measurements was studied during a French-Italian meeting (Admirat et al., 1980). The data for 6 hailfalls (3 on the French network and 3 on the Italian, 99 plates total) were reexamined by several operators. The distribution of relative energy deviations thus obtained from different measures is shown in Figure (2). As with sampling errors, these deviations between two independent realizations will be accounted for by a purely random noise of maximum amplitude  $DEd = 0.4 E$ .

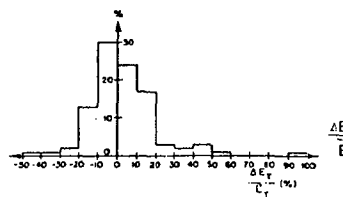


Fig. 2. Distribution of relative energy deviations from several operators

The measurement error due to calibration essentially induces a variation in diameter class determination. Following the hailstone dimensional spectrum, the error is more or less carried on to the kinetic energy. In practice

these variations are evaluated in the same way as those of dent measurements, the latter being also mainly due to dent shift from one class to another.

The error due to hailpad saturation occurs only with high energy density. Of all hailpads used in the test, less than 2% are considered as being saturated and then energy density may be underestimated by as much as 50% (Waldvogel et al., 1978). After an initial random high density selection, we remove from E a random quantity of between 0.5 E and 0.

By superposing over the value  $E(x,y)$ , a complex noise taking into account these different error sources, we obtained at each hailpad station a "measured" energy density  $E_T(x,y)$ .

We calculate global energy measured by:

$$E_G = s \sum_{i=1}^P E_{Ti}(x,y) \quad (s \text{ being the mesh area})$$

The mesh area  $S_G$  being given by  $S_G = s P$ .

Figure 3 reproduces the result of random samples on a square network (10 x 10) with a 3.8 km<sup>2</sup> mesh. These hailpatterns all have the same "true" global energy  $E_R = 20$  MJ and the same area  $S_R = 5.6$  km<sup>2</sup>. The measured energies vary between 7 MJ and 58 MJ with an average measured area of 5.7 km<sup>2</sup>.

P	valeurs de $E_{Ti}$	(J/m <sup>2</sup> )	$E_G$ (MJ)
2	14.30	1.02	58.23
1	6.59		25.03
1	12.90	0.79	49
1	8.46		32.14
2	1.80	1.03	9.86
1	1.86		7.07
2	1.86	2.99	10.98
1	11.73		42.67
2	4.09	2.92	26.91
2	3.96		26.14

$\bar{S}_G = 5.7 \text{ km}^2$                        $\bar{E}_G = 28.8 \text{ MJ}$

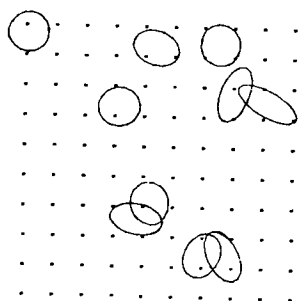


Fig. 3. Example of the result of 10 random hail-patterns ( $E_R = 20$  MJ;  $S_R = 5.6$  km<sup>2</sup>)

### 3.3 Hailfall climatology consideration

For each value  $E_R$  we make 500 random hail-

pattern selections and each time we evaluate the corresponding measured area  $S_G$  and global energy  $E_G$ .

The distribution of the conditional probability of measuring  $E_G$  from a hailpattern of "true" energy  $E_R$ , i.e.  $P_{E_R}(E_G)$ , is thus obtained. With a series of values  $E_R$  covering the natural variation interval, a stochastic matrix  $\Pi_E$  characterizing the global energy network response can be constituted. Each line of the matrix  $\Pi_E$  correspond to a value  $E_R$  and gives for each energy class  $E_G$ , the probability  $P_{E_R}(E_G)$ . To be complete this natural hail-

fall simulation must note the climatologic frequency with which each "true" global energy value  $E_R$  can be produced on the network. An estimation of this "a priori" climatologic frequency distribution  $P(E_R)$  can be evaluated from the "a posteriori" frequency distribution of measured energies and from  $\Pi_E$  (Doras, 1982).

From the estimated "a priori" frequency distribution  $P(E_R)$  and the matrix  $\Pi_E$ , we can now determine in a simple manner  $P_{E_G}(E_R)$ , i.e. the

conditional law of probability,  $E_G$  being know the "true" energy is  $E_R$ . For this we can multiply each line of  $\Pi_E$  by the adequate climatologic probability and  $P_{E_G}(E_R)$  will be given (following normalization) in the  $E_G$  column.

## 4. RESULTS AND VALIDITY

### 4.1 Results

For a network user who determines the hailed station P number and the measured global energy  $E_G$ , the problem is to know the most probable values  $S_R$  and  $E_R$  and their standard errors. For that we use probability distributions  $P_{E_G}(E_R)$ . They are nearly symmetric, the average value  $E_R$  remaining close to the measured value  $E_G$  and the standard deviation  $E_R$  increasing regularly with  $E_G$ .

Fig. 4 shows the logarithmic scales, the standard "true" energy error  $\sigma \bar{E}_R / \bar{E}_R$  in terms of measured  $E_G$  for three network grids (1km<sup>2</sup>, 3.8 km<sup>2</sup> and 8 km<sup>2</sup> meshes).

For Grossversuch (3.8 km<sup>2</sup> mesh) the regression line is:

$$\sigma \bar{E}_R / \bar{E}_R = 3.18 E_G^{-0.505} \quad (E_G \text{ in MJ}).$$

Waldvogel and Schmid (1981) obtained similar results from Grossversuch IV radar recordings. They found the same square root decrease for the standard measured error of  $\sigma E_G / E_G$  but with greater values (by an approximate factor of 2) than those from simulation ( $\sigma E_G / E_G$  is the standard error of the values  $E_G$  corresponding to the same "true" value  $E_R$ ; it can be calculated from  $P_{E_R}(E_G)$  dis-

tributions and its variation is found to be very close than those of  $\sigma E_R / E_R$ ).

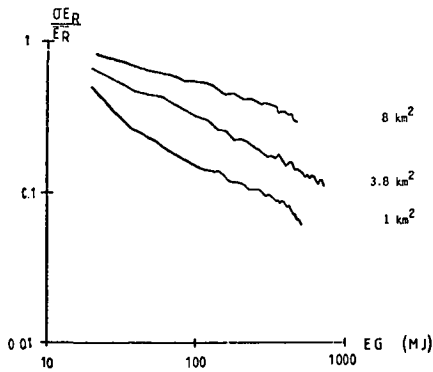


Figure 4. Standard error variations versus  $E_G$

During the simulation, it is also possible to take out a matrix  $\Pi_S$  which is the area network response, i.e. with fixed value of  $E_R$  (therefore of  $S_R$ ) being known, we have a conditional probability distribution of measured area  $S_G$ ,  $P_{SR}(S_G)$ . This matrix  $\Pi_S$  with an estimated area climatology leads to an evaluation for each value  $S_G$  of the most probable value  $S_R$  ( $\bar{S}_R$ ) with a standard deviation  $\sigma_{S_R}$ . The standard error  $\sigma_{S_R}/\bar{S}_R$  decreases progressively with the number of hailed stations and the correspondent regression line is:

$$\sigma_{S_R}/\bar{S}_R = 0.5 P^{-0.71}$$

This result is the same regardless of the network grid used (provided that the mesh is smaller than the most frequent hailpattern area).

#### 4.2 Comparison with observations

To test the model's ability to represent hail-pattern realities we give on a diagram  $\log S_G/\log E_G$  (Figure 5), on one hand, the true measurement of natural hailfalls (indicated by circles) and, on the other hand, the results of a simulation made from a similar sample of values  $E_R$  (indicated by crosses). As we can see, the model values (+) offer a great dispersion relative to the experimental curve used to calculate the model. This dispersion covers a large part, but not all, of that of natural hailpatterns (70% to 80%). It therefore appears that the hailpattern model and the measurement simulation method already offer an interesting approach to many of the Grossversuch IV natural hailfall properties and variabilities. However the fact that there still remains an under estimation of this variability shows the limits of this representation.

To improve it we can try to take into account the fine scale variability as well as the diameter class punctual errors. Also, in order to reestablish a more dispersed physical reality, we can give the model an additional flexibility concerning the regression relations. Trials to improve the model in this sense have been made. They give a better natural variability representation and the results concerning the energy measurement error are comparable to those of Waldvogel and Schmid.

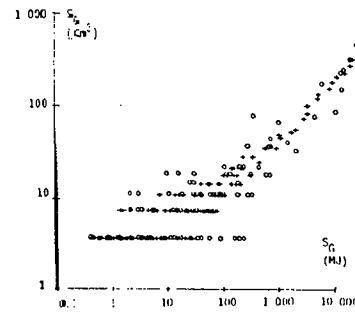


Figure 5. Comparison of natural (o) and modelled (+) hailpatterns

#### 5. CONCLUSION

The study presented here and its first results already suggest a global evaluation for hailpad network measurement errors. For Grossversuch IV a minimum error limit is given by the relation:  $\sigma_{E_R}/E_R = 3.18 E_G^{-0.505}$ . A finer evaluation seems to be obtained through a more complete and flexible model.

The simulation method developed on this occasion offers a certain number of advantages. It is thus possible, using a  $\Pi_E$  matrix established with the logarithmic variation steps, to examine the effects of measurement errors in the Grossversuch IV test. A first application of this transformation leads to test results which are hardly influenced by measurement errors.

The simulation method is also a tool to make a model for the global hailfall process and its measurements on a given network. This permits us, for example to test *a priori* which energy density distribution modifications, for a given climatology, are or are not apt to bring about sensitive test experience effects. Studies of this kind would certainly be interesting before undertaking any costly scientific experiments.

#### REFERENCES

- Admirat P., D. Vento, J.F. Mezeix, J.P. Rouet, and A. Aparo, 1980: *Atmos Ocean*, 18 (1), 27-42.
- Doras N., 1982: Rapport Technique G.N.E.F.A., n° 42, Valence.
- Gertzman, H.S. and D. Atlas, 1977: *J. Geoph. Res.* 82, 4955-4977.
- Joss J., and A. Waldvogel, 1969: *J. Atmos. Sci.* 26, 566-569.
- Long, A.B., 1978: *Atmos Ocean*, 16 (1), 35-48.
- Lozowski E.P. and G.S. Strong, 1978: *J. Appl. Meteor.*, 17, 521-528.
- Mezeix, J.F. and P. Admirat, 1978: *Atmos Ocean*, 16 (1) 61-68.
- Mezeix, J.F. and N. Doras, 1981: *J. Appl. Meteor.* 20, 377-385.
- Morgan, G.M. and N.G. Towery, 1975: *J. Appl. Meteor.*, 14, 763-769.
- Waldvogel A., B. Federer, W. Schmid and J.F. Mezeix, 1978: *J. Appl. Meteor.*, 17, 1680-1693.
- Waldvogel A., and W. Schmid, 1981: Preprints 20th Conf. Rad. Meteor., AMS, Boston, 187-193.
- Wojtiw L., and E.P. Lozowski, 1978: *Atmos Ocean*, 16 (1), 17-34.